Langmuir

Letter

pubs.acs.org/Langmuir

Synthesis of Janus Nanoparticles via a Combination of the Reversible Click Reaction and "Grafting to" Strategies

Junting Li, Lei Wang, and Brian C. Benicewicz*

Department of Chemistry and Biochemistry, University of South Carolina, Columbia, South Carolina 29208, United States

Supporting Information

ABSTRACT: A critical challenge in nanoparticle functionalization has been the preparation of polymer-grafted asymmetric (Janus) nanoparticles (diameter < 100 nm). We describe a robust and cyclic method involving a reversible click reaction and "grafting to" strategies to synthesize such nanoparticles. Mechanochemistry was used in a protection−deprotection process to separate nanoparticles cleanly that were anchored to larger particles, and the recovered azide-functionalized larger particles could be recycled as face-blocking moieties. With this combination of strategies, we prepared 15 nm silica nanoparticles that were partially functionalized with poly(methyl methacrylate). Additionally, the unique self-assembly behaviors of the resultant Janus nanoparticles were investigated in different solvents at different concentrations.

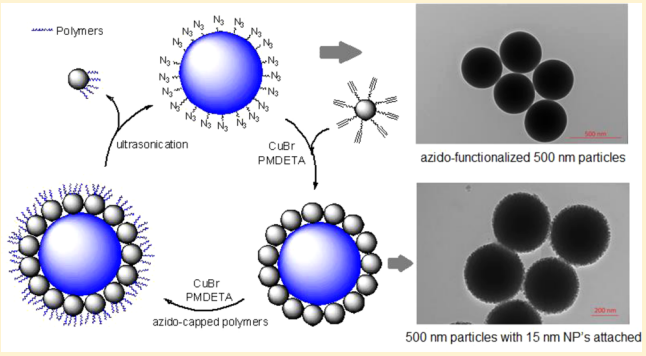

INTRODUCTION

Asymmetrical particles (also named Janus particles), including spatially asymmetric particles[1−4] and spherical particles carrying asymmetric functionalities, impart anisotropic properties with unique self-assemblies and thus have many potential applications, such as phase-transfer or multistep catalysts, multitargeted drug carriers, and bioimaging agents.[5−7] In this Letter, our discussion focuses on the latter type of Janus particles. A number of strategies have been developed for the synthesis of Janus particles starting with isotropic particles[8] in which the most crucial step is temporarily or permanently masking a portion of their surface either by biphasic interaction[9,10] or by monolayer coating.[11,12] Nevertheless, most of these reported methods were based on relatively large particles (with diameters greater than 100 nm) due to limitations of the techniques. Additionally, modifying Janus particles with small-molar-mass ligands is still the most common synthesis route. In contrast, growing polymer brushes on inorganic nanoparticles (NPs) is of great interest because polymers can have a more significant influence on the properties of NPs. By controlling the chemistry of the grafted polymers, graft densities, and polymer chain lengths, the morphology of the NPs in matrices[13,14] and their mechanical properties[15,16] can be precisely tuned. The strategies for uniformly modifying NPs with polymer brushes can be categorized into "grafting from"[17,18] and "grafting to".[19] However, it is still challenging to apply these strategies to produce Janus NPs, and only a few groups have reported the successful syntheses of polymer-grafted Janus NPs.[20−22]

With many new mechanophore structures developed in recent years, mechanochemistry has become a very powerful tool for organic synthesis and advanced material design[23−27] because it enables many chemical transformations that cannot occur through thermal or photochemical stimuli (e.g., the cycloreversion of the triazole ring formed by azide and alkyne in the copper-mediated click reaction, which has widely broadened the application of this classic reaction and made it an efficient pathway to reversible covalent connections[28]). However, the majority of these reactions to date have relied only on polymer materials to activate bond cleavages mechanically.

Herein, we describe a novel, mechanochemically driven, and cyclic approach to the fabrication of polymer-grafted Janus NPs by combining the reversible click reaction and grafting to strategies. This approach harnesses mechanical forces to unclick and cleave the particle−particle attachment selectively, although the copper-mediated click reaction for NP connections has already been reported.[22] Silica particles with an average diameter of 500 nm were chosen as substrates to immobilize silica NPs with an average diameter of 15 nm on their surfaces. Considering the relatively small size, the 500 nm silica particles have a much larger specific surface area than planar substrates,[10,11,20] thus more NPs could be partially masked with the same volume of substrates. Moreover, they are easy to synthesize, precipitate, and redisperse in various solvents, and these properties simplified the experimental operations. Detailed experimental procedures are provided in the Supporting Information.

Received: May 27, 2013
Revised: September 3, 2013
Published: September 3, 2013

ACS Publications © 2013 American Chemical Society

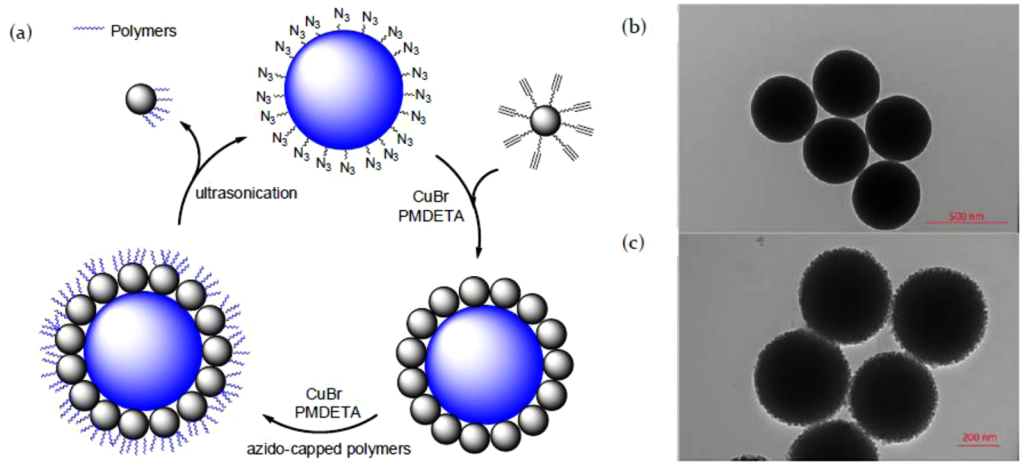

Figure 1. (a) Schematic illustration of the cyclic synthesis route for polymer-grafted Janus silica NPs by combining the reversible click reaction and grafting to strategies. (b) TEM image of azido-functionalized 500 nm particles. (c) TEM image of 500 nm particles with 15 nm NPs attached.

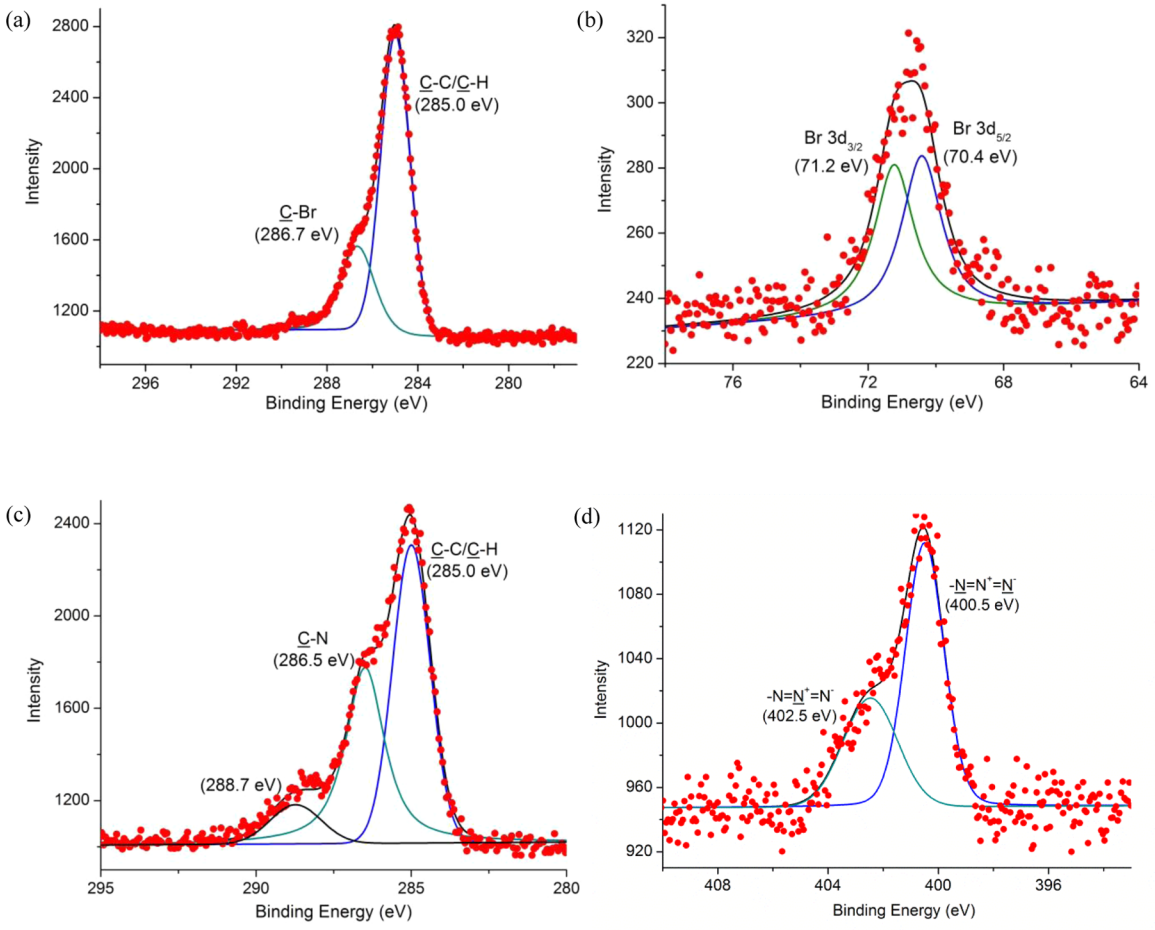

Figure 2. (a) C 1s and (b) Br 3d core-level XPS spectra of bromo-functionalized 500 nm particles. (c) C 1s and (d) N 1s core-level XPS spectra of azido-functionalized 500 nm particles. Binding energies are calibrated to aliphatic carbon at 285.0 eV.

RESULTS AND DISCUSSION

The cyclic synthesis route is depicted in Figure 1a. First, the surfaces of 500 nm particles (Figure 1b) and 15 nm NPs were functionalized by azido and alkynyl groups, respectively. Then the 15 nm NPs were attached to the surface of the 500 nm particles via the copper-mediated click reaction (Figure 1c). All free 15 nm NPs were removed in a repeated centrifugation–dispersion process, noting that the 500 nm particles can be precipitated in DMF under centrifugation at 5000 rpm, but the 15 nm NPs remain suspended. Next, azido-capped poly(methyl methacrylate) (N_3-PMMA) was added to the suspension of the particle complexes in DMF, and the exposed surface of the 15 nm NPs was modified by N_3-PMMA through a click reaction again using a grafting to strategy. Finally, the PMMA-grafted Janus NPs were released under sonication, and the 500 nm particles could be recycled for another round of attachment.

dx.doi.org/10.1021/la401990d | *Langmuir* 2013, 29, 11547–11553

Because of the low surface to volume ratio of the 500 nm particles, the surface functionalities were difficult to detect through conventional methods, such as FT-IR and NMR, even though excess amounts of 3-bromo propyltrimethoxysilane and sodium azide were added in each step to maximize the graft densities. An azide absorption was displayed as a barely perceptible peak at 2120 cm^{-1} in the FT-IR spectrum of the azido-functionalized particles (Figure s1a). Thus, X-ray photoelectron spectroscopy (XPS) was utilized to confirm the surface functionalities of the 500 nm particles. XPS analysis of the bromo-functionalized particles verified the presence of C 1s and Br 3d (Figure 2a,b). The C 1s region was observed as two overlapping peaks with binding energies of 286.7 and 285.0 eV that were assigned to *C*-Br and *C*-H/*C*-C groups, respectively. A more distinctive bromine peak was observed at 70.8 eV consisting of Br $3d_{5/2}$ and Br $3d_{3/2}$ components. After the conversion of bromide to azide, the N 1s region appeared as two slightly merged peaks at 402.5 and 400.5 eV with an expected peak area ratio of 1:2 (Figure 2d) corresponding to the N^+ and N^- species of azide on the surface. The emergence of the two peaks was consistent with previous observations because of the degradation of azide under X-ray exposure.[29] In addition, both of the peaks of *C*-N (286.5 eV) and *C*-C/*C*-H (285.0 eV) were observed in the C 1s region (Figure 2c), and the other peak with binding energy of 288.7 eV was attributed to the degradation of azide. Therefore, the XPS analysis verified the functionalization and conversion of the groups on the surface of the 500 nm particles.

In contrast, the alkynyl functionalization of 15 nm NPs was easily verified by the absorption at 3323 cm^{-1} ascribed to C≡CH in the FT-IR spectrum (Figure s1b), and UV−vis spectra were used to calculate the alkyne graft densities as shown in the Supporting Information. In this experiment, silica NPs with high graft density (0.7 alkyne/nm^2) were synthesized first. However, in the following step, it was difficult to break the attachment between these NPs and 500 nm azido-functionalized particles under sonication for more than 1 h. It was hypothesized that too many "triazole" linkages were formed between the surfaces attributed to the high graft densities, and the ultrasound was not effective enough to cleave all of the bonds. When NPs with a graft density of 0.4 alkyne/nm^2 were used for the procedure, most of the resultant Janus NPs could be released after sonication for 30 min.

The click reaction generated covalent linkages between the particles, which were much stronger than noncovalent absorptions,[8,19] reducing the chance that the NPs might be washed away from the surface of the substrates during processing. A controlled reaction was carried out between the two sizes of particles without the copper(I) bromide catalyst, which showed that attachment did not occur after overnight stirring. It was previously reported that the chain scission of polymers through the mechanochemical "unclick" reaction was dependent on the molecular weights of the polymer blocks.[28] Thus, it is easier to break a 1,2,3-triazole ring if the masses on both sides of the ring are heavier. Because the particles used in this study were much heavier than individual polymer chains, the cleavage occurred readily. Additionally, collision and friction between the particles during sonication may have assisted the cleavage. It is worth noting that after collection by centrifugation the 500 nm particles were ready to react with alkynyl-functionalized NPs again without any further treatments, and similar particle complexes were obtained as observed in the first round, indicating that the azido groups on the particle surface had been recovered.

The N_3-PMMA for Janus NP modification was synthesized via RAFT polymerization using an azido-functionalized chain-transfer agent. To enhance the selectivity of the "unclick" reaction and prevent the risk that the grafted polymers might be removed from the surfaces during sonication, polymers with low molecular weights (PMMA: M_n = 13.3K, PDI = 1.11) and short ultrasound times (within 1 h) were applied. After the treatment with azido-capped PMMA, the FT-IR spectrum of the PMMA-grafted Janus NPs revealed a characteristic absorption of PMMA (Figure s1c, e.g., 1732 cm^{-1} ascribed to the carbonyl groups), which indicated the attachment of the polymer. TEM images also showed that there were significant changes on the surface of the particle complex (Figure s2). However, the asymmetric geometry of individual Janus NPs cannot be observed by TEM because of their small size.

In addition, a contrast test was designed to demonstrate the partial functionalization of the Janus NPs: 500 nm particles with an attachment of 15 nm NPs were used in one group, and free alkyne-functionalized NPs were in the other group with the same graft density (0.4 alkyne/nm^2) and amount as the attached NPs. Both of them were treated with identical N_3-PMMA solution in DMF though the copper-mediated click reaction. After workup, PMMA-functionalized Janus NPs and uniform NPs were produced, respectively. The NPs were subjected to TGA analysis, which showed that the Janus NPs exhibited an overall weight loss of 24% whereas the uniform NPs exhibited an overall weight loss of 35% (Figure 3).

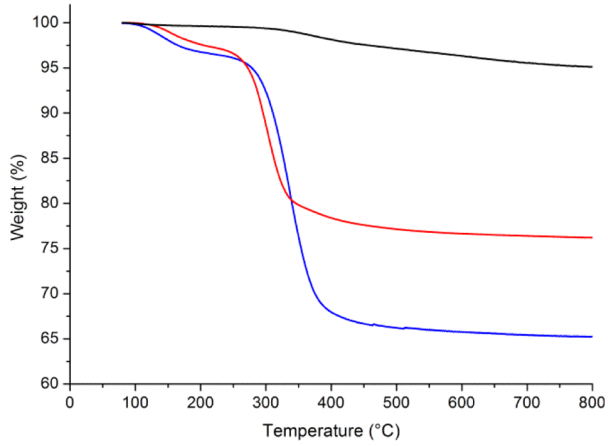

Figure 3. TGA scans of alkyne-functionalized NPs (black), PMMA-grafted Janus NPs (red), and PMMA-grafted uniform NPs (blue).

Considering the weights of the alkynyl-functionalization and other small-molar-mass impurities, the calculation indicated that the Janus NPs had about 16 wt % of PMMA grafted and that uniform NPs had 26 wt % of PMMA. Under similar reaction conditions, the two groups of NPs should have similar polymer graft densities if all reaction sites are available. Accordingly, a reasonable explanation for the smaller amount of PMMA on the Janus NPs was that its surface had been only partially modified.

Although their anisotropic properties cannot be demonstrated by observing individual NPs, the PMMA-grafted Janus NPs were dispersed with unique self-assembly behaviors that were investigated by TEM in different solvents and concentrations. Initially, when the sample was prepared with

dx.doi.org/10.1021/la401990d | *Langmuir* 2013, 29, 11547−11553

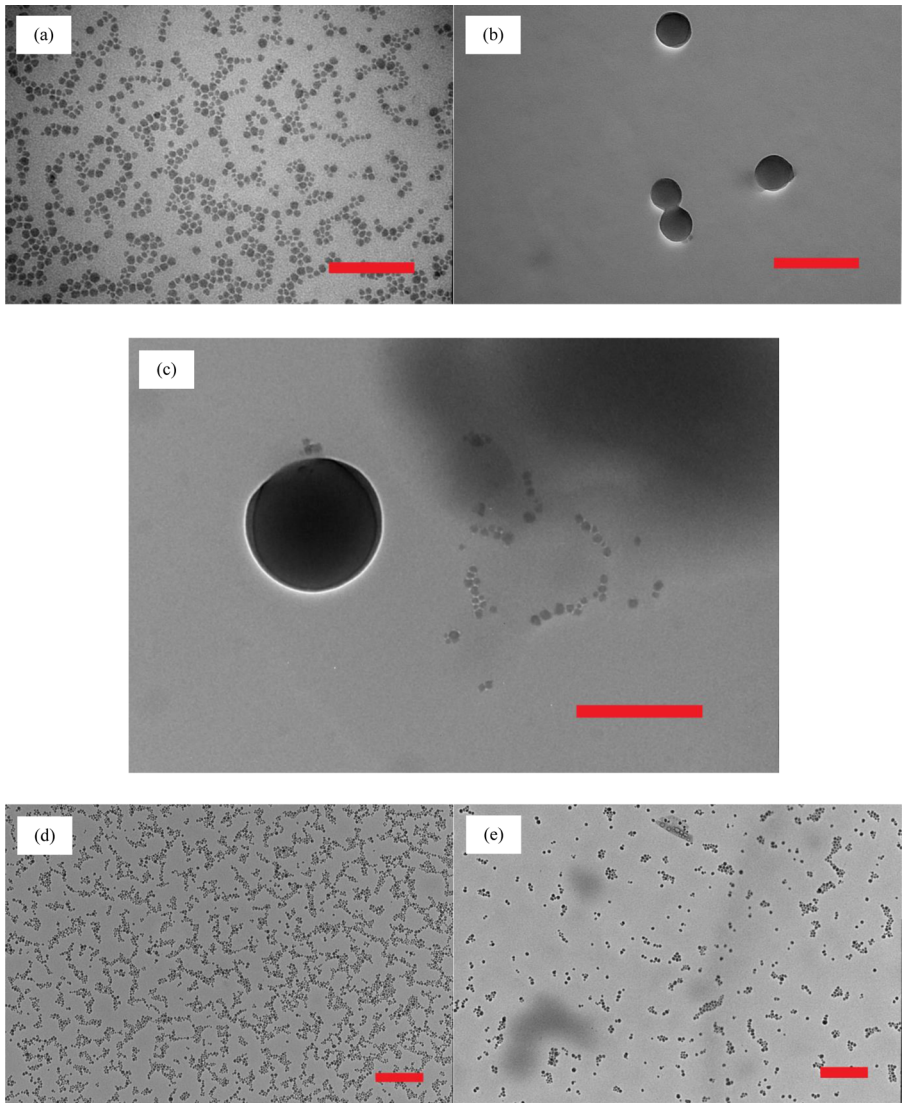

Figure 4. TEM images of (a) PMMA-grafted Janus NPs (15 nm) in THF (3.1 mg/mL), (b) PMMA-grafted Janus NPs (15 nm) in THF (0.62 mg/mL), (c) micelle formed by PMMA-grafted Janus NPs (15 nm) in THF (0.62 mg/mL) (close-up view), (d) alkynyl-functionalized non-Janus NPs (15 nm) in THF (3.0 mg/mL), and (e) alkynyl-functionalized non-Janus NPs (15 nm) in THF (0.60 mg/mL). The scale bars in a–c are 200 nm, and the scale bars in d and e are 500 nm.

3.1 mg/mL of PMMA-grafted NPs in THF, individual NPs were displayed in the TEM image (Figure 4a). Next, micelle-like structures in a range from 50 to 200 nm were detected when the solution was diluted to 0.62 mg/mL (Figure 4b,c). Higher resolutions did not provide much additional information because of the thickness of the collapsed micelle, similar to other TEM results on nanoparticle micelle structures.[30] This self-assembly was probably due to the different solubilities of the two faces of the Janus NPs. Because the PMMA-grafted Janus NPs have both solvophilic and solvophobic faces, it was logical to assume that they can act as nanosurfactants in solution. Nevertheless, unlike the critical micelle concentration of molecular surfactants, our observation implied that there was a maximum limit of concentration for the Janus NPs beyond which micelles cannot be formed. Such self-assemblies were not observed in the samples of non-Janus NPs (alkyne-functionalized NPs) with different concentrations in THF (Figure 4d,e).

When samples of the PMMA-grafted Janus NPs were prepared in DMF, individual NPs could always be observed regardless of the concentrations. The different behaviors of the Janus NPs in THF and DMF were also verified by AFM analysis (Figure s3). The AFM image of the THF sample showed that the center of the round structures was thicker and softer and their edge was thinner and harder, presumably from deformed micelles resulting from the drying effect.

Another experiment was conducted using both Janus and non-Janus NPs. When alkynyl-functionalized non-Janus NPs in DMF (0.4 alkyne/nm^2, 0.3 mg/mL) were gradually added to the solution of PMMA-grafted Janus NPs at the same concentration, a series of very interesting mutations of NP dispersions were displayed in the TEM analysis. Starting from the homogeneous dispersion of pure Janus NPs (Figure 5a), micelle-like structures were detected immediately after the addition of a few drops of the non-Janus NPs solution (Figure 5b). A reasonable explanation is that the Janus NPs behaved as nanosurfactants and covered the non-Janus NPs to form micelles ascribed to their better solubility and asymmetric properties. Then the micelle-like structures disappeared with the sample containing about 15% of the non-Janus NPs.

dx.doi.org/10.1021/la401990d | *Langmuir* 2013, 29, 11547–11553

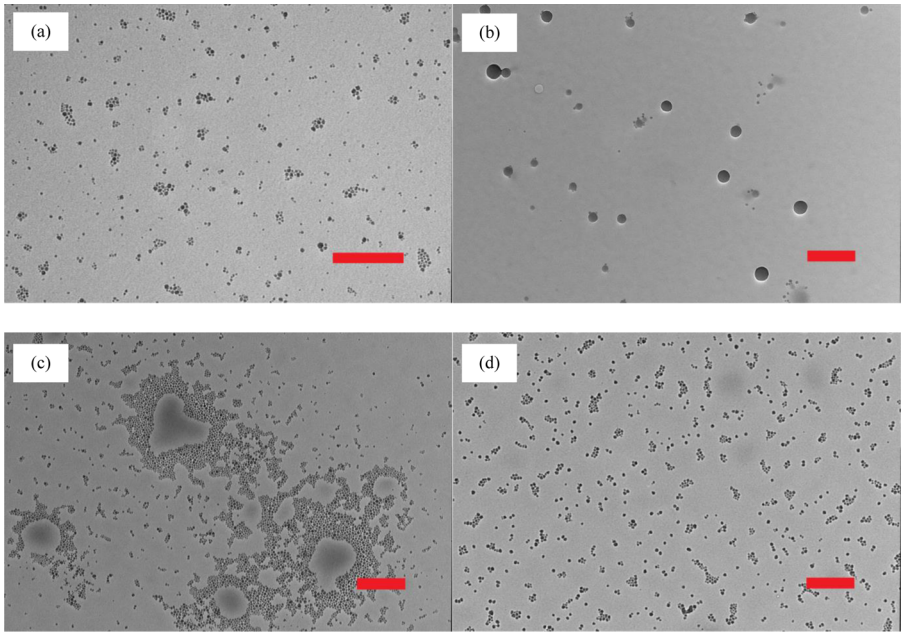

Figure 5. TEM images showing the dispersion changes (a–d) of the PMMA-grafted Janus NPs in DMF (0.3 mg/mL) with a gradual addition of alkynyl-functionalized NPs (0.3 mg/mL). The scale bars are 500 nm.

Instead, the NPs were arranged around a few cyclical areas (Figure 5c). This dispersion might be attributed to the collapse of the unstable micelles because not enough Janus NPs were available to cover the whole surface when more non-Janus NPs were added. Eventually, when the proportion of the non-Janus NPs was high enough (>50%), the NP rings vanished completely, and only single NPs and NP clusters could be detected (Figure 5d), which was similar to the dispersion of pure Janus NPs.

■ EXPERIMENTAL SECTION

(Please refer to the Supporting Information for experimental details and characterizations.)

Preparation of Silica Particles (500 nm). Silica particles (500 nm) were prepared through the Stober process: ammonia (29%, 10 mL), distilled water (11 mL), and ethanol (75 mL) were mixed in a round-bottom flask at first, and then tetraethyl orthosilicate (TEOS) was added all at once under stirring at 500 rpm. After an overnight reaction, the resultant silica particles were washed through a multiple dispersion–centrifugation process. Finally, 1.77 g of silica particles as a white powder was obtained after drying in a vacuum oven at room temperature.

Preparation of Azido-Functionalized Silica Particles (500 nm). Silica particles (500 nm, 1.77 g) were added to a three-necked round-bottomed flask with 3-bromopropyltrimethoxysilane (0.73 g, 3.0 mmol) and dried THF (300 mL). The reaction mixture was held at 75 °C under nitrogen protection overnight and then cooled to room temperature. The product was washed through a multiple dispersion–centrifugation process. In the last round, the bromo-functionalized silica particles were redispersed in 200 mL of DMF and added to a three-necked round-bottomed flask together with sodium azide (0.39 g, 6.0 mmol) and distilled water (15 mL). The reaction mixture was held at 80 °C overnight and then cooled to room temperature. The product was washed through a multiple dispersion–centrifugation process. Finally, the particles were dispersed in DMF for the further use.

Activation of 5-Hexynoic Acid. 5-Hexynoic acid (500 mg, 4.46 mmol), 2-mercaptothiazoline (532 mg, 4.46 mmol), and dicyclohexylcarbodiimide (DCC) (1.11 g, 5.35 mmol) were dissolved in 20 mL of dichloromethane. (Dimethylamino)pyridine (DMAP) (54 mg, 0.45 mmol) in 5 mL of dichloromethane was added slowly to the solution, which was stirred at room temperature for 6 h. The solution was filtered to remove the salt. After the removal of solvent and silica gel column chromatography (3:2 hexane/ethyl acetate), activated 5-hexynoic acid was obtained as a light-green oil (903 mg, 95% yield).

Preparation of Alkynyl-Functionalized Silica Nanoparticles (15 nm). A THF solution (30 mL) of amino-functionalized silica nanoparticles (2.70 g) was added dropwise to a THF solution (30 mL) of activated 5-hexynoic acid (0.50 g, 2.3 mmol) at room temperature. After complete addition, the solution was stirred for 6 h. The reaction mixture was then precipitated into a large amount of 4:1 cyclohexane/ethyl ether (500 mL). The particles were recovered by centrifugation at 3000 rpm for 15 min. The particles were then redissolved in 30 mL of THF and reprecipitated in 4:1 cyclohexane/ethyl ether. This dissolution–precipitation procedure was repeated another two times. Nanoparticles (2.91 g) as a light-yellow powder were obtained after drying in a vacuum oven at room temperature.

Synthesis of 6-Azidohexyl 4-Cyano-4-(phenylcarbonothioylthio)pentanoate (Azido-Functionalized CPDB). CPDB (878 mg, 3.15 mmol), 1-azido-6-hydroxyhexane (500 mg, 3.49 mmol), and DCC (720 mg, 3.49 mmol) dissolved in 30 mL of DMAP (128 mg, 1.05 mmol) in 5 mL of dichloromethane were added slowly to the solution, which was stirred at room temperature overnight. The solution was filtered to remove the salt. After the removal of solvent and silica gel column chromatography (10:1 hexane/ethyl acetate), azido-functionalized CPDB was obtained as a dark-red oil (798 mg, 63% yield).

Synthesis of Azido-Capped Poly(methyl methacrylate) (N_3-PMMA). A solution of MMA (1.0 g, 10 mmol), azido-functionalized CPDB (13.4 mg, 33 μmol), V-70 (3.3 μmol), and THF (1.0 mL) was prepared in a dried Schlenk tube. The mixture was degassed by three freeze–pump–thaw cycles, backfilled with nitrogen, and then placed in an oil bath at 40 °C for 15 h. The polymerization solution was quenched in ice water, and the resultant azido-capped polymer was precipitated in hexane. Molecular weight characteristics were analyzed by GPC.

Preparation of Janus Nanoparticles via Reversible Click Reaction. Azido-functionalized silica particles (500 nm, 0.4 g), alkynyl-functionalized silica nanoparticles (15 nm, 80 mg) and *N*,*N*,*N*′,*N*′,*N*″-pentamethyldiethylenetriamine (PMDETA) (0.5 μL, 2 μmol) were dissolved in DMF (50 mL). The mixture was degassed by flushing with nitrogen for 30 min, and then CuBr (0.3 mg, 2 μmol) was added. After a 1 day reaction under nitrogen protection at room

dx.doi.org/10.1021/la401990d | *Langmuir* 2013, 29, 11547–11553

temperature, the suspensions were washed through a multiple dispersion−centrifugation process. The precipitated 500 nm particles with 15 nm nanoparticles attached were collected, redispersed in DMF (50 mL), and added to a three-necked flask with azido-capped PMMA (7.2 μmol) and a trace amount of PMDETA. After 30 min of nitrogen flushing, a trace amount of CuBr was added for another 1 day click reaction. Finally, the unreacted PMMA was removed by centrifugation at 5000 rpm, and the particle complexes were redispersed in THF. The suspension was ultrasonicated for 1 h and sequentially centrifuged at 3000 rpm for 15 min and filtered. The Janus nanoparticles were obtained in the liquid phase.

CONCLUSIONS

We designed a facile and cyclic method to synthesize polymer-grafted Janus NPs. A novel mechanochemical approach was introduced into the particle interactions to achieve the protection−deprotection process of NPs selectively and was used in combination with the polymer modification of the unprotected surfaces of the NPs by a grafting to strategy. Although silica NPs were used as a template in the current experiments, this approach is universal and can be performed on NPs of various materials to introduce asymmetric surface coverage as long as their surfaces are properly functionalized. Moreover, our research demonstrated that NPs could be another type of material suitable for mechanochemistry in addition to polymers. Preliminary investigations of the unique self-assembly behaviors of the polymer-grafted Janus NPs were conducted by TEM and AFM in different solvents and concentrations, implying their potential applications as nano-surfactants.

ASSOCIATED CONTENT

Supporting Information

Figures relevant to the discussion and experimental procedures for the synthesis and characterization of PMMA-grafted nanoparticles. This material is available free of charge via the Internet at http://pubs.acs.org.

AUTHOR INFORMATION

Corresponding Author

*Fax: +001 803 777 8100. Tel: +001 803 777 0778. E-mail: benice@sc.edu.

Author Contributions

J.L. conducted the experiments and characterized the materials. L.W. contributed suggestions and prepared samples for characterization. B.C.B. wrote the grant that supported the work, originated the research idea with the main ideas, and supervised the work. The manuscript was written through the contributions of all authors. All authors have given approval to the final version of the manuscript.

Notes

The authors declare no competing financial interest.

ACKNOWLEDGMENTS

The authors acknowledge financial support from the South Carolina SmartState Centers of Economic Excellence program.

REFERENCES

(1) Reculusa, S.; Poncet-Legrand, C.; Perro, A.; Duguet, E.; Bourgeat-Lami, E.; Mingotaud, C.; Ravaine, S. Hybrid Dissymmetrical Colloidal Particles. *Chem. Mater.* **2005**, *17*, 3338−3344.

(2) Yin, Y.; Zhou, S.; You, B.; Wu, L. Facile Fabrication and Self-Assembly of Polystyrene−Silica Asymmetric Colloid Spheres. *J. Polym. Sci., Polym. Chem.* **2011**, *49*, 3272−3279.

(3) Liu, B.; Liu, J.; Liang, F.; Wang, Q.; Zhang, C.; Qu, X.; Li, J.; Qiu, D.; Yang, Z. Robust Anisotropic Composite Particles with Tunable Janus Balance. *Macromolecules* **2012**, *45*, 5176−5184.

(4) Jia, L.; Zhou, F.; Liu, W. Janus Nanoparticle Magic: Selective Asymmetric Modification of Au-Ni Nanoparticles for Its Controllable Assembly onto Attapulgite Nanorods. *Chem. Commun.* **2012**, *48*, 12112−12114.

(5) de Gennes, P.-G. Soft Matter (Nobel Lecture). *Angew. Chem., Int. Ed.* **1992**, *31*, 842−845.

(6) Jiang, S.; Chen, Q.; Tripathy, M.; Luijten, E.; Schweizer, K. S.; Granick, S. Janus Particle Synthesis and Assembly. *Adv. Mater.* **2010**, *22*, 1060−1071.

(7) Hu, J.; Zhou, S.; Sun, Y.; Fang, X.; Wu, L. Fabrication, Properties and Applications of Janus Particles. *Chem. Soc. Rev.* **2012**, *41*, 4356−4378.

(8) Perro, A.; Reculusa, S.; Ravaine, S.; Bourgeat-Lami, E.; Duguet, E. Design and Synthesis of Janus Micro- and Nanoparticles. *J. Mater. Chem.* **2005**, *15*, 3745−3760.

(9) Hong, L.; Jiang, S.; Granick, S. Simple Method to Produce Janus Colloidal Particles in Large Quantity. *Langmuir* **2006**, *22*, 9495−9499.

(10) Wang, F.; Phonthammachai, N.; Mya, K. Y.; Tjiua, W. W.; He, C. PEG-POSS Assisted Facile Preparation of Amphiphilic Gold Nanoparticles and Interface Formation of Janus Nanoparticles. *Chem. Commun.* **2011**, *47*, 767−769.

(11) Zhao, Z.; Shi, Z.; Yu, Y.; Zhang, G. Ternary Asymmetric Particles with Controllable Patchiness. *Langmuir* **2012**, *28*, 2382−2386.

(12) Tang, J. L.; Schoenwald, K.; Potter, D.; White, D.; Sulchek, T. Bifunctional Janus Microparticles with Spatially Segregated Proteins. *Langmuir* **2012**, *28*, 10033−10039.

(13) Akcora, P.; Liu, H.; Kumar, S. K.; Moll, J.; Li, Y.; Benicewicz, B. C.; Schadler, L. S.; Acehan, D.; Panagiotopoulos, A. Z.; Pryamitsyn, V.; Ganesan, V.; Ilavsky, J.; Thiyagarajan, P.; Colby, R. H.; Douglas, J. F. Anisotropic Self-Assembly of Spherical Polymer-Grafted Nanoparticles. *Nat. Mater.* **2009**, *8*, 354−359.

(14) Dukes, D.; Li, Y.; Lewis, S.; Benicewicz, B. C.; Schadler, L. S.; Kumar, S. K. Conformational Transitions of Spherical Polymer Brushes: Synthesis, Characterization, and Theory. *Macromolecules* **2010**, *43*, 1564−1570.

(15) Akcora, P.; Kumar, S. K.; Moll, J.; Lewis, S.; Schadler, L. S.; Li, Y.; Benicewicz, B. C.; Sandy, A.; Narayanan, S.; Ilavsky, J.; Thiyagarajan, P.; Colby, R. H.; Douglas, J. F. Gel-like Mechanical Reinforcement in Polymer Nanocomposite Melts. *Macromolecules* **2010**, *43*, 1003−1010.

(16) Gao, J.; Li, J.; Benicewicz, B. C.; Zhao, S.; Hillorg, H.; Schadler, L. S. The Mechanical Properties of Epoxy Composites Filled with Rubbery Copolymer Grafted SiO_2. *Polymers* **2012**, *4*, 187−210.

(17) Pyun, J.; Jia, S.; Kowalewski, T.; Patterson, G. D.; Matyjaszewski, K. Synthesis and Characterization of Organic/Inorganic Hybrid Nanoparticles: Kinetics of Surface-Initiated Atom Transfer Radical Polymerization and Morphology of Hybrid Nanoparticle Ultrathin Films. *Macromolecules* **2003**, *36*, 5094−5104.

(18) Li, C.; Han, J.; Ryu, C. Y.; Benicewicz, B. C. A Versatile Method to Prepare RAFT Agent Anchored Substrates and the Preparation of PMMA Grafted Nanoparticles. *Macromolecules* **2006**, *39*, 3175−3183.

(19) Lupitskyy, R.; Motornov, M.; Minko, S. Single Nanoparticle Plasmonic Devices by the "Grafting to" Method. *Langmuir* **2008**, *24*, 8976.

(20) Lattuada, M.; Hatton, T. A. Preparation and Controlled Self-Assembly of Janus Magnetic Nanoparticles. *J. Am. Chem. Soc.* **2007**, *129*, 12878−12889.

(21) Wang, B.; Li, B.; Zhao, B.; Li, C. Y. Amphiphilic Janus Gold Nanoparticles via Combining "Solid-State Grafting-to" and "Grafting-from" Methods. *J. Am. Chem. Soc.* **2008**, *130*, 11594−11595.

(22) Zhang, S.; Li, Z.; Samarajeewa, S.; Sun, G.; Yang, C.; Wooley, K. L. Orthogonally Dual-Clickable Janus Nanoparticles via a Cyclic Templating Strategy. *J. Am. Chem. Soc.* **2011**, *133*, 11046−11049.
(23) Diesendruck, C. E.; Steinberg, B. D.; Sugai, N.; Silberstein, M. N.; Sottos, N. R.; White, S. R.; Braun, P. V.; Moore, J. S. Proton-Coupled Mechanochemical Transduction: A Mechanogenerated Acid. *J. Am. Chem. Soc.* **2012**, *134*, 12446−12449.
(24) Wiggins, K. M.; Brantley, J. N.; Bielawski, C. W. Polymer Mechanochemistry: Force Enabled Transformations. *ACS Macro Lett.* **2012**, *1*, 623−626.
(25) Groote, R.; Jakobs, R. T. M.; Sijbesma, R. P. Performance of Mechanochemically Activated Catalysts Is Enhanced by Suppression of the Thermal Effects of Ultrasound. *ACS Macro Lett.* **2012**, *1*, 1012−1015.
(26) Kean, Z. S.; Black Ramirez, A. L.; Yan, Y.; Craig, S. L. Bicyclo[3.2.0]heptane Mechanophores for the Non-Scissile and Photochemically Reversible Generation of Reactive Bis-Enones. *J. Am. Chem. Soc.* **2012**, *134*, 12939−12942.
(27) Cravotto, G.; Cintas , P. Harnessing mechanochemical effects with ultrasound-induced reactions. *Chem. Sci.* **2012**, *3*, 295−307.
(28) Brantley, J. N.; Wiggins, K. M.; Bielawski, C. W. Unclicking the Click: Mechanically Facilitated 1,3-Dipolar Cycloreversions. *Science* **2011**, *333*, 1606−1609.
(29) Hansen, T. S.; Larsen, N. B. Conductive Polymer Functionalization by Click Chemistry. *Macromolecules* **2008**, *41*, 4321−4327.
(30) Starmans, L. W. E.; Burdinski, D.; Haex, N. P. M.; Moonen, R. P. M.; Strijkers, G. J.; Nicolay, K.; Grüll, H. Iron Oxide Nanoparticle-Micelles (ION-Micelles) for Sensitive (Molecular) Magnetic Particle Imaging and Magnetic Resonance Imaging. *PLOS ONE* **2013**, *8*, e57335.